Calretinin-immunoreactivity during Postnatal Development of the Rat Isocortex: a Qualitative and Quantitative Study

G. S. Schierle, J.-C. Gander, C. D'Orlando, M. R. Celio and D. M. Vogt Weisenhorn

Institute of Histology and General Embryology, University of Fribourg, CP 100, 1705 Fribourg, Switzerland

Postnatal development of the rat cortex is characterized by the gradual development of many calcium-dependent processes which demand a precise control of the intracellular levels of this cation; when the balance is disturbed, neuronal death ultimately ensues. Calretinin (CR), a calcium-binding protein, has been postulated to have a neuroprotective capacity by buffering intracellular calcium. This putative relationship between CR and neuroprotection is still, however, a controversial issue. With a view to shedding further light on this subject, we studied the temporal and spatial distribution of CR in five different regions (the frontal-, sensorimotor-, parietal-, temporal- and occipital region) of the rat cortex during postnatal development. Qualitative and quantitative immunocytochemistry of newborn, 5-, 10-, 15-, 20- and 30-day-old and adult rats revealed a profound increase in the density of CR-positive neurons during the first two postnatal weeks in all regions examined. At the end of this period, CR-immunoreactive cells decreased sharply to adult levels. Cell classes exhibiting transient CR-immunoreactivity during the first two postnatal weeks included cells in layer I (amongst which were Cajal–Retzius cells), the subplate and pyramidal-like cells in the upper portion of layer V, most of them found in the motor cortices. The above-described dynamics of CR expression were reflected also in the biochemical analysis performed (immunoblotting, ELISA). The temporal and spatial correlation with calcium-dependent events such as synaptogenesis, neurite elongation and remodelling further support the contention that CR may play a neuroprotective role during postnatal development of the rat cortex.

Intracellular calcium plays a key role in many processes during the development of the central nervous system. It has been shown to be involved in cell division, neuronal migration, neurite extension, synaptogenesis, the development of neuronal excitability, neuronal plasticity and coactivation of neuronal domains (Campbell, 1983; Kater *et al.*, 1988; Komuro and Rakic, 1992; Spitzer *et al.*, 1994; Yuste *et al.*, 1995). The performance of such diverse functions necessarily entails a precise regulation of the levels of this cation. When these rise above a certain critical limit, as occurs for example after prolonged stimulation with excitatory amino acids, neurite outgrowth is inhibited, dendrites are stunted and cell death ultimately follows (Mattson and Kater, 1987, 1989; Choi, 1988; Lipton, 1989). One possible strategy of neurons to limit excessive rises in intracellular calcium leading to neuronal death could be the presence of proteins capable of buffering intracellular calcium, such as the calcium-binding proteins parvalbumin (Pauls *et al.*, 1996), calbindin-D28k (Hunziker and Schrickel, 1988) and its closest homologue CR (Rogers, 1987; Parmentier, 1990). They may serve a neuroprotective role, but such a notion has still to be put on a firm footing (McDonald and Johnston, 1990; Mattson *et al.*, 1991; Chard *et al.*, 1993; Hof *et al.*, 1993; Freund and Magloczky, 1993; Iacopino *et al.*, 1994; Lukas and Jones, 1994; Möckel and Fischer, 1994; Vogt Weisenhorn *et al.*, 1996; for review see Heizmann and Braun, 1995).

Parvalbumin, calbindin-D28k and CR are widely distributed in the central nervous system and have proved, despite their unknown function, to be excellent neuroanatomical markers in the adult as well as in the developing brain (for review see Andressen *et al.*, 1993; Heizmann and Braun, 1995). Each of these calcium-binding proteins is located in the adult cortex within subsets of inhibitory neurons and they manifest strikingly different patterns of distribution during development.

Parvalbumin appears very late during cortical development and displays a very specific pattern of distribution. It has therefore been implicated in the maturation of cortical inhibitory circuits and/or the onset of experience-dependent activity (Stichel *et al.*, 1987; Seto-Ohshima *et al.*, 1990; Hendrickson *et al.*, 1991; Solbach and Celio, 1991; Sánchez *et al.*, 1992; Alcántara *et al.*, 1993; Hogan and Berman, 1994; Alcántara and Ferrer, 1994). Calbindin-D28k, on the other hand, appears very early and exhibits a transient, region-specific pattern of expression (Enderlin *et al.*, 1987; Hendrickson *et al.*, 1991; Liu and Graybiel, 1992; Sánchez *et al.*, 1992; Alcántara *et al.*, 1993; Hogan and Berman, 1993). Temporal correlation with calcium-dependent events during development suggests a role in the onset of thalamocortical interactions and cortical plasticity in the monkey (Hendrickson *et al.*, 1991). It has also been suggested that calbindin-D28k is involved in cell movement and the formation of neuronal processes (Enderlin *et al.*, 1987).

The distribution pattern of CR during development has been assessed only in the somatosensory cortex of the rat (Vogt Weisenhorn *et al.*, 1994, 1996; Fonseca *et al.*, 1995) and the visual cortex of the monkey (Yan *et al.*, 1995a,b). In the former, CR is expressed very early during cortical development (embryonic day 11) with a transient increase during early postnatal development. As a consequence of this finding, it was proposed that this calcium-binding protein is involved in processes such as neurite elongation and synaptogenesis; during embryogenesis, an involvement in neuronal migration was also suggested.

If, during postnatal development, CR is indeed involved in such general cortical developmental events, its temporal and spatial distribution pattern should be similar in all neocortical regions. Therefore, in the present study we expanded the former studies concerning the distribution of CR during the postnatal development of the neocortex of the rat to four additional cortical regions (the frontal-, sensorimotor-, temporal- and occipital region) and furnished quantitative data from three regions (the frontal-, parietal- and occipital region). We also determined the content of CR in the entire neocortex at the defined stages of development by ELISA and immunoblotting.

Cerebral Cortex Mar 1997;7:130–142; 1047–3211/97/$4.00

Materials and Methods

Immunocytochemistry

Sixteen rats of either sex were killed on the day of birth (P0; n = 2), or postnatal day 5 (P5; n = 2), 10 (P10; n = 2), 15 (P15; n = 2), 20 (P20; n = 4) or 30 (P30; n = 2), or as an adult (n = 2). Animals were asphyxiated with CO_2 and the brains perfused via the heart initially with saline (0.9%) at 37°C and then with 4% paraformaldehyde in phosphate buffer (pH 7.4) at 4°C. The brains were then rapidly removed from the skull, cryoprotected first with 18% and then with 25% sucrose in Tris-buffered saline (TBS), and subsequently frozen in liquid nitrogen.

Serial cryostat sections, 50 µm in thickness, were cut in the coronal plane and collected in 0.1 M TBS. Free-floating sections were incubated with a polyclonal antibody against CR [CR 7969 (Schwaller *et al.*, 1993); diluted 1:5000 in TBS containing 10% bovine serum] at 4°C for 3 days. They were then exposed to biotinylated goat anti-rabbit IgG (Vector; dilution of 1:200, 2 h) and later to avidin–biotin peroxidase complex (Vectastain ABC kit, Vector; dilution of 1:100, 3 h). The peroxidase reaction was visualized using 0.05% diaminobenzidine and 0.01% hydrogen peroxide. False positive immunoreactions were excluded by incubating a few tissue sections without the primary antibody. As a control for the specificity of the antiserum, sections derived from two P20 animals were incubated with a polyclonal antiserum against chicken CR (a gift of J. Rogers; Rogers, 1987). Every third section was stained with cresyl violet (Nissl stain) in order to ascertain the boundaries of cortical layers and areas (Zilles and Wree, 1985).

CR-immunoreactivity was assessed qualitatively in five cortical regions (the frontal-, hind limb-, parietal-, temporal- and occipital region). In six sections per animal, the density of CR-immunoreactive neurons was determined quantitatively in the parietal-, frontal- and occipital region. The number of intensely labelled neurons was counted within 200 μm^2 grids throughout the entire depth of the developing cortex, the forbidden and permitted borderline positions being respected (Williams and Rakic, 1988, 1989). The volumes of the different cortices were measured and cell counts were normalized and expressed as number of cells/mm^3. Statistical comparison of data was performed using a non-parametric (Mann–Whitney) test.

Immunoblotting

Rat cortices at defined stages of development [P0 (n = 3), P5 (n = 1), P10 (n = 1), P15 (n = 3), P20 (n = 1), P30 (n = 1) and adult (n = 3)] were dissected out, homogenized in the presence of EDTA and proteinase inhibitors, and centrifuged at 14 000 g for 30 min at 4°C. Protein samples from each extract were separated by SDS–PAGE and transferred onto Hybond-ECL membranes (Amersham). These were saturated with 5% non-fat milk in TBS and 0.1% Tween-20 for 1 h at room temperature and then incubated with rabbit polyclonal antibody CR 7969 in the same solution (1:2000) at 4°C overnight. The membranes were rinsed in TBS containing 0.1% Tween-20 and incubated for 2 h in the milk buffer with a peroxidase-coupled goat anti-rabbit IgG [1:2000 (Sigma)]. After thorough washing, the membranes were further processed according to the protocol for enhanced chemoluminescence detection (ECL- Amersham). In order to exclude the possibility of detecting different conformational forms of CR due to a different calcium-binding status, additional immunoblotting was performed under calcium-free conditions; i.e. all solutions including the extracts contained 10 mM EDTA.

ELISA

Rat cortices at defined stages of development [P0 (n = 2), P5 (n = 1), P10 (n = 1), P15 (n = 2) and adult (n = 2)] were dissected out, homogenized in 1% proteinase inhibitor cocktail and centrifuged. The salt concentration was adjusted to 150 mM using 5 M NaCl. To enrich the calcium-binding proteins in the supernatants, samples were heated at 60°C for 1 min and again centrifuged. The clear supernatants containing soluble proteins were stored at –20°C until required for ELISA, which was performed for each extract in triplicate.

We used a sandwich ELISA method. Purified goat-anti-CR antibody [20 mg/ml in a solution containing 20 mM Tris–HCl (pH 7.5), 150 mM NaCl, 0.02% (v/v) Kathon and 10 mg/l amaranth] was diluted (1:1000) in 100 mM $NaHCO_3$ (pH 9.5). A 96-well plate was coated with this solution (200 µl/well) and incubated for 16–24 h at room temperature. Following a twofold washing step in water, each well was saturated with 200 µl of 0.2 M Tris–HCl (pH 7.5) containing 1% (w/v) bovine serum albumin (BSA) and 0.02% (v/v) Kathon for 24 h and then again rinsed with water.

In order to establish a standard curve, a stock solution of purified recombinant CR [1 µg/ml CR (Schwaller *et al.*, 1993) in a solution containing 0.1 M phosphate buffer (pH 6.5), 0.5% (w/v) BSA and 0.02% (v/v) Kathon was diluted in 0.2 M Tris–HCl (pH 7.5), containing 0.5% (w/v) BSA, 0.02% (v/v) Kathon and 0.1% (w/v) phenol, to give the following amounts of CR (in 50 µl): 0, 30, 62, 125 and 250 pg. Aliquots (50 µl) of each solution were dispensed into each well. Brain extracts containing soluble proteins were diluted in the same solution and 50 µl/well added. Each sample was measured in triplicates. The incubation with the samples lasted for 24 h at 4°C. Wells were then washed twice with 0.05% (v/v) Tween-20 and twice with water. One volume of the second antiserum (CR 7969) was mixed with one volume of 0.1 M Tris–HCl (pH 7.5) containing 0.5% (w/v) BSA, 0.02% (v/v) Kathon, 0.1% (w/v) phenol and 10 mg/l Evans Blue. The resulting solution was then diluted (1:1000) in 0.2 M Tris–HCl (pH 7.5) containing 0.5% (w/v) BSA, 0.02% (v/v) Kathon and 0.1% (w/v) phenol. Next, 50 µl of the diluted antiserum was added to each well. After an incubation period of 24 h the wells were washed as described above, then 50 µl of a goat anti-rabbit peroxidase serum (diluted 1:40 000 in the same solution as for the second antiserum) was added to each well. Incubation was carried out for 24 h at 4°C, followed by thorough washing (see above). To visualize the bound peroxidase 200 µl of a TMB–peroxide solution [20 mM 3,3′,5,5′- tetramethylbenzidine and 50 mM hydrogen peroxide in 10% (v/v) acetone and 90% (v/v) ethanol] was added to each well. Development of the blue reaction product was arrested by adding 100 µl of 1 M sulphuric acid per well and its absorbance was measured photometrically at 450 nm.

Results

The expression profile of CR-immunoreactivity in the rat cortex has been assessed qualitatively during both pre- and postnatal stages of development only in the parietal region (Vogt Weisenhorn *et al.*, 1994, 1996; Fonseca *et al.*, 1995). In the current study, we expanded this study and evaluated its developmental distribution in four additional cortical regions (the frontal-, sensorimotor-, temporal- and occipital region) using a polyclonal antiserum (CR 7969). We derived corroborative quantitative data (density of CR-immunoreactive neurons) pertaining to three cortical regions (the frontal-, parietal- and occipital region). We also determined the CR-content of the cortex as a function of postnatal development by immunoblotting and ELISA.

Qualitative Analysis of CR-immunoreactivity

Day of Birth (P0)

On the day of birth, CR-immunoreactivity was pronounced in each of the regions examined (Figs 1–5). CR-immunoreactive neurons were found throughout the entire depth of the developing cortex. Large numbers of intensely stained neurons were observed particularly in layer I and the subplate (Fig. 6*A*,*G*). These two layers were also conspicuous because of their intensive staining in the neuropil. Most of the CR-positive neurons located within the subplate manifested a multipolar morphology, whereas in layer I, many stained neurons had only one prominent dendrite, which was horizontally oriented. This is typical for Cajal–Retzius cells. Many CR-immunoreactive neurons were also found within the cortical plate, which is interposed between layer I and the subplate (Fig. 6*D*). They were mostly located principally at the level of the emanating layer V. The morphology of these cells was very heterogeneous, both horizontally and vertically oriented neurons being encountered. The latter were mostly bipolar in appearance and it was thus

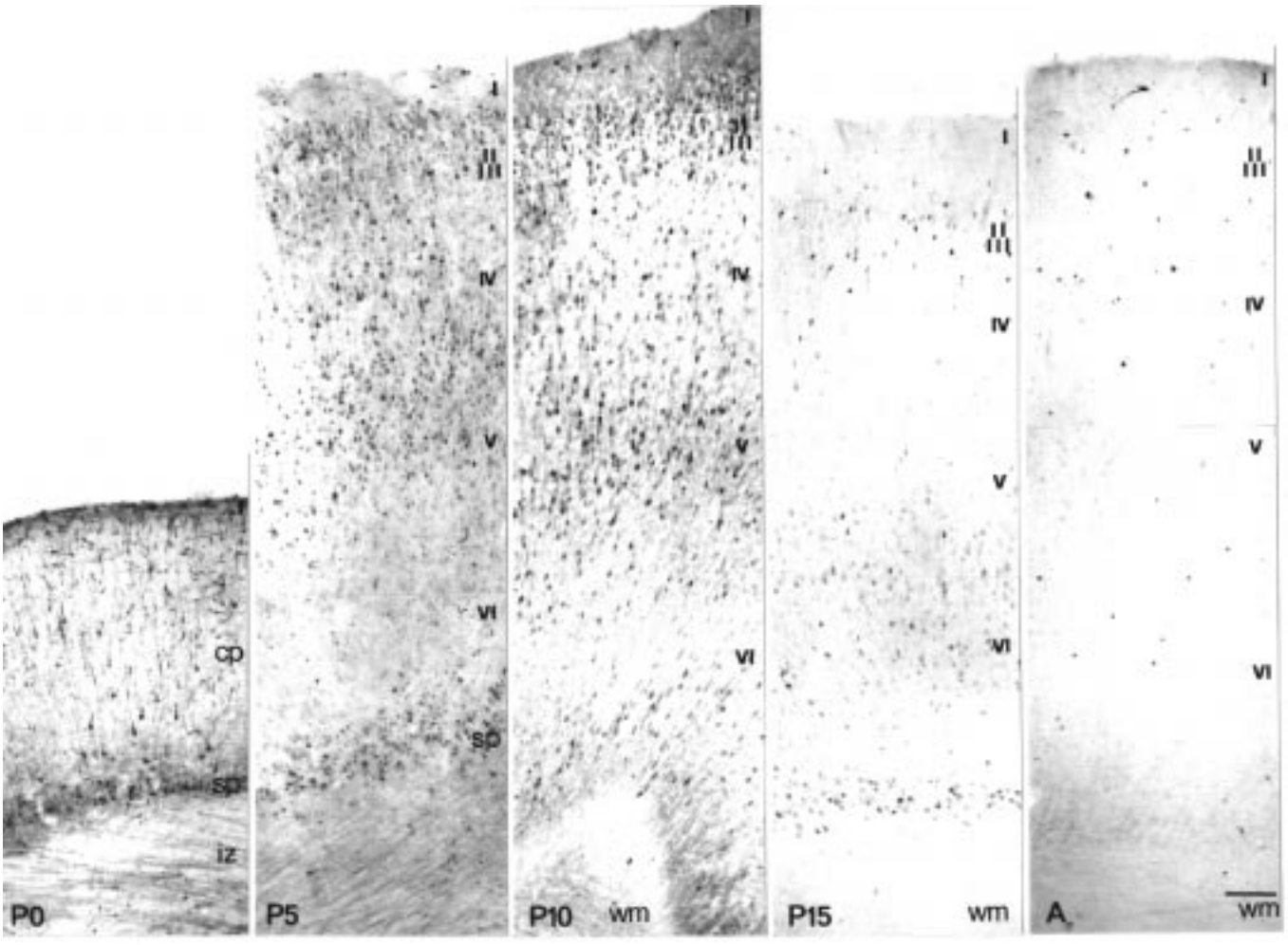

Figure 1. CR-immunoreactivity in the *frontal* region of rat isocortex on the day of birth (P0), on postnatal days 5 (P5), 10 (P10) and 15 (P15), and in the adult (A). Note particularly the many faintly stained neurons in layer II and in the upper portion of layer III on P5 and P10. cp = cortical plate; sp = subplate; wm = white matter; cortical layers (I–VI) are indicated. Scale bar = 120 μm.

difficult to ascertain whether these were maturing cells or neurons which were still migrating to their final destination. Some pyramidal-like cells were also found, located especially in the lower portion of the emerging cortical plate. Immunoreactive neurons were also abundant in the intermediate and ventricular zones. They were multipolar and horizontal oriented. Cells immediately adjacent to the ventricles exhibited a simple morphology, and often protruded only one short dendrite. Some immunoreactive fibres were observed within the intermediate zone. They were more abundant underneath the parietal cortex than under the other examined cortical regions. In all examined regions the distribution of CR-immunoreactivity throughout the depth of the cortical plate was largely the same. No major differences could be observed.

Five-day-old Rats

In layer I and the subplate a fair number of CR-positive neurons could be found (Figs 1–5 and 6*B*,*H*). The neuropil staining was still present. However, the intensity of the subplate staining was decreased compared with the day of birth, probably due to its starting disintegration. The cortical plate had thickened and many CR-immunoreactive bipolar and multipolar neurons were found in the emerging upper layers. In layer V the number of stained pyramidal-like cells had increased (Fig. 6*E*). A number of faintly stained neurons exhibiting a similar morphology were also encountered in the supragranular layers. There was a striking topographic variation in the number of pyramidal-like cells. They were observed at the highest densities in the sensorimotor region. They were also conspicuous in the parietal,

Figure 2. CR-immunoreactivity in the *hindlimb* region of rat isocortex on the day of birth (P0), on postnatal days 5 (P5), 10 (P10) and 15 (P15), and in the adult (A). Note the intensely stained pyramidal-like cells in the upper portion of layer V. cp = cortical plate; sp = subplate; wm = white matter; cortical layers (I–VI) are indicated. Scale bar = 120 μm.

Figure 3. CR-immunoreactivity in the *parietal* region of rat isocortex on the day of birth (P0), on postnatal days 5 (P5), 10 (P10) and 15 (P15), and in the adult (A). Note the obtrusiveness of the neuropil and the intensely stained pyramidal-like neurons in the upper portion of layer V. cp = cortical plate; sp = subplate; wm = white matter; cortical layers (I–VI) are indicated. Scale bar = 120 μm.

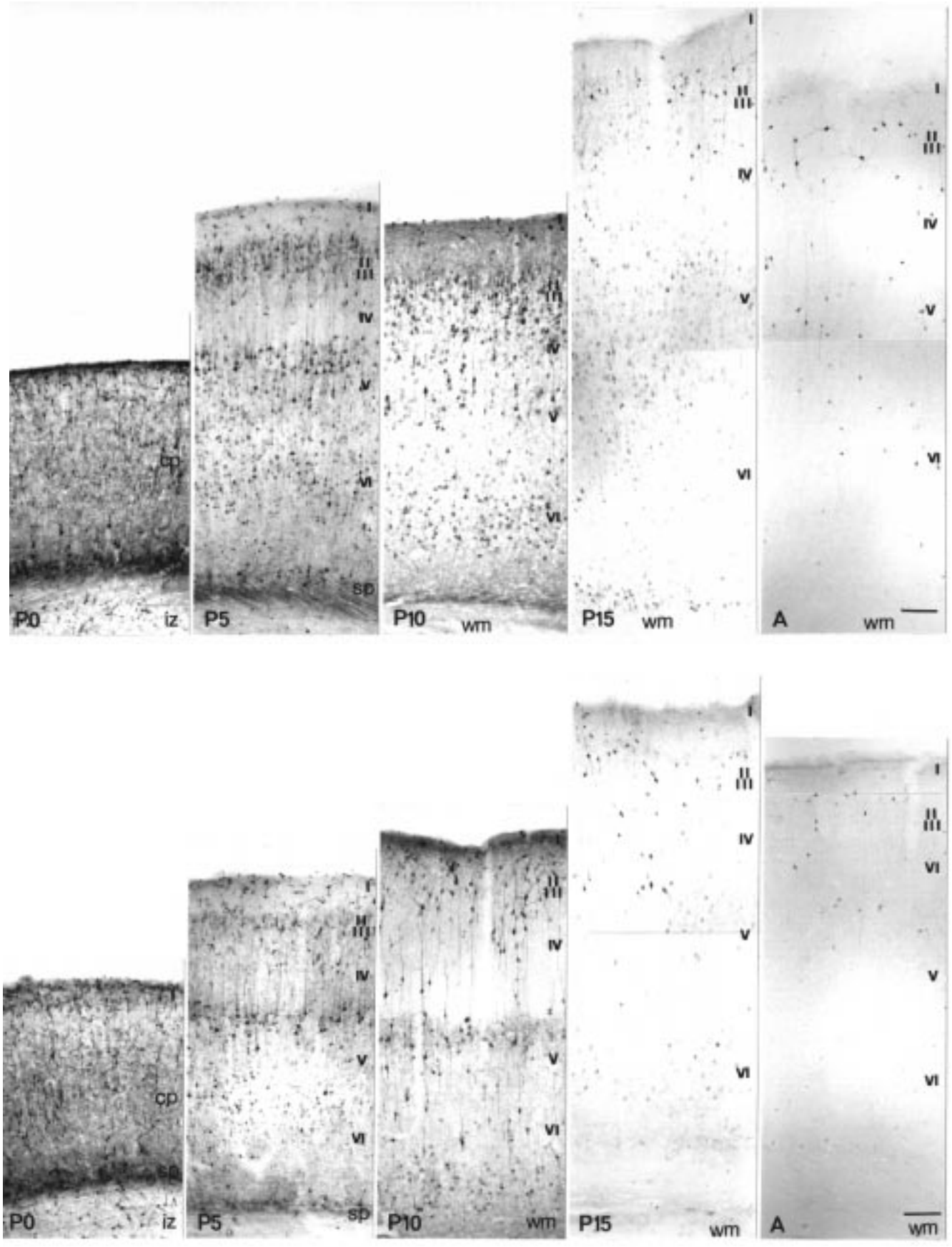

Figures 2 and 3

frontal and temporal regions. In the occipital region relatively few were observed.

Ten-day-old Rats

Ten days after birth, many immunoreactive cells of varying staining intensity were found in layers II, III, V and VI (Figs 1–5). Many intensely stained multipolar and vertically oriented neurons were observed. Most of the latter exhibited either bipolar or bitufted morphologies (Fig. 6*F*). In the upper portion of layer V CR-positive pyramidal-like neurons were still apparent, but their density was somewhat reduced in comparison with the situation observed on P5. In contrast to the general tendency of increasing numbers of CR-immunoreactive neurons, in layer I the number of immunoreactive neurons had decreased compared with P5 (Fig. 6*C*). Furthermore, the immunoreactivity due to the neuropil staining in the subplate had disappeared (Fig. 6*I*) and was not replaced by an equivalent staining in layer VIb. Some immunoreactive fibres and cells were observed in the white matter.

At this stage of development, differences in the distribution profile of CR-immunoreactive neurons were apparent within each of the cortical regions examined (Figs 1–5). In the frontal region the immunoreactive neurons were dispersed fairly equally throughout the depth of the cortex, with a paucity within layer IV (Fig. 1). The hindlimb region was remarkable for the amount of immunoreactivity within layer II and the upper portion of layer III (Fig. 2). In the parietal and temporal regions, staining in layers II and III was less intense than in the hindlimb region (Figs 3 and 4). Staining of the neuropil in the upper portion of layer V (Va) was, however, more pronounced and manifested as a distinct band in the middle of the cortex. In the occipital region, staining of the neuropil at this level was barely visible (Fig. 5).

Fifteen-day-old Rats

The distribution profile of CR-immunoreactivity changed considerably between P10 and P15 (Figs 1–5). In all layers the overall staining was much lower on P15. In layer I only a few multipolar neurons and some horizontally oriented ones were immunoreactive (Fig. 7*A*). Most of the CR-immunoreactive nerve cells were located in the supragranular layers and displayed bipolar, bitufted and also multipolar morphologies (Fig. 7*D*,*G*), indicating that the adult distribution pattern had been attained. In layer V very faintly stained neurons, only a minority of which manifested a pyramidal morphology, were observed. Intensely stained immunoreactive pyramidal cells were, however, still found in the cingulate cortex (Fig. 7*F*). In the frontal and hindlimb regions faint CR-immunoreactivity was still observed in layer VIb. The neuropil staining in layer I and upper portion of layer V had diminished. Some immunoreactive neurons were always encountered within the underlying white matter.

Twenty- and Thirty-day-old and Adult Rats

The distribution patterns of CR-immunoreactivity manifested on P20 and P30 were strikingly similar to that observed in adult rats. The number of immunoreactive neurons was very low and virtually all of those were intensely stained. They were encountered within each layer but tended to be concentrated in the supragranular layers (Figs 1–5). The majority had a distinctly bipolar or bitufted morphology (Fig 7*E*,*I*). Some multipolar neurons were also found (Fig 7*H*). A few faintly stained pyramidal cells were encountered in the upper portion of layer V

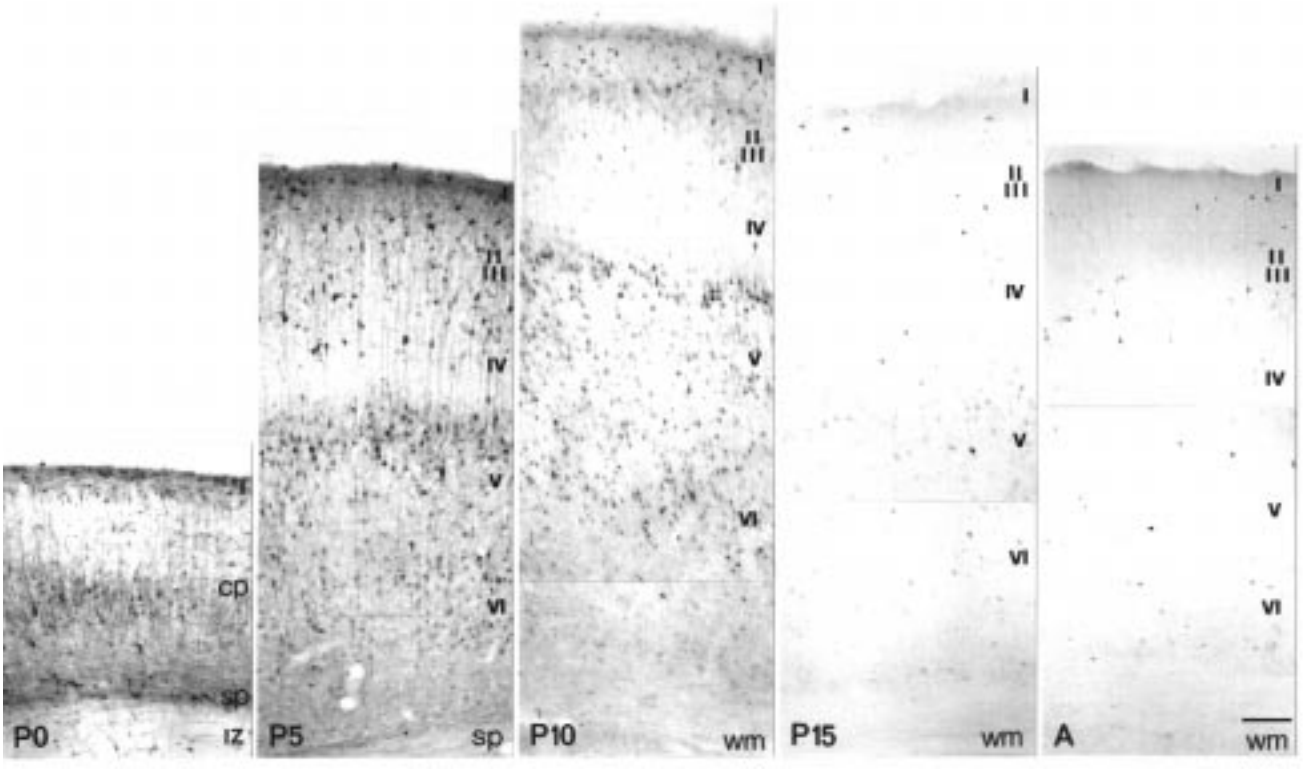

Figure 4. CR-immunoreactivity in the *temporal* region of rat isocortex on the day of birth (P0), on postnatal days 5 (P5), 10 (P10) and 15 (P15), and in the adult (A). cp = cortical plate; sp = subplate; wm = white matter; cortical layers (I–VI) are indicated. Scale bar = 120 μm.

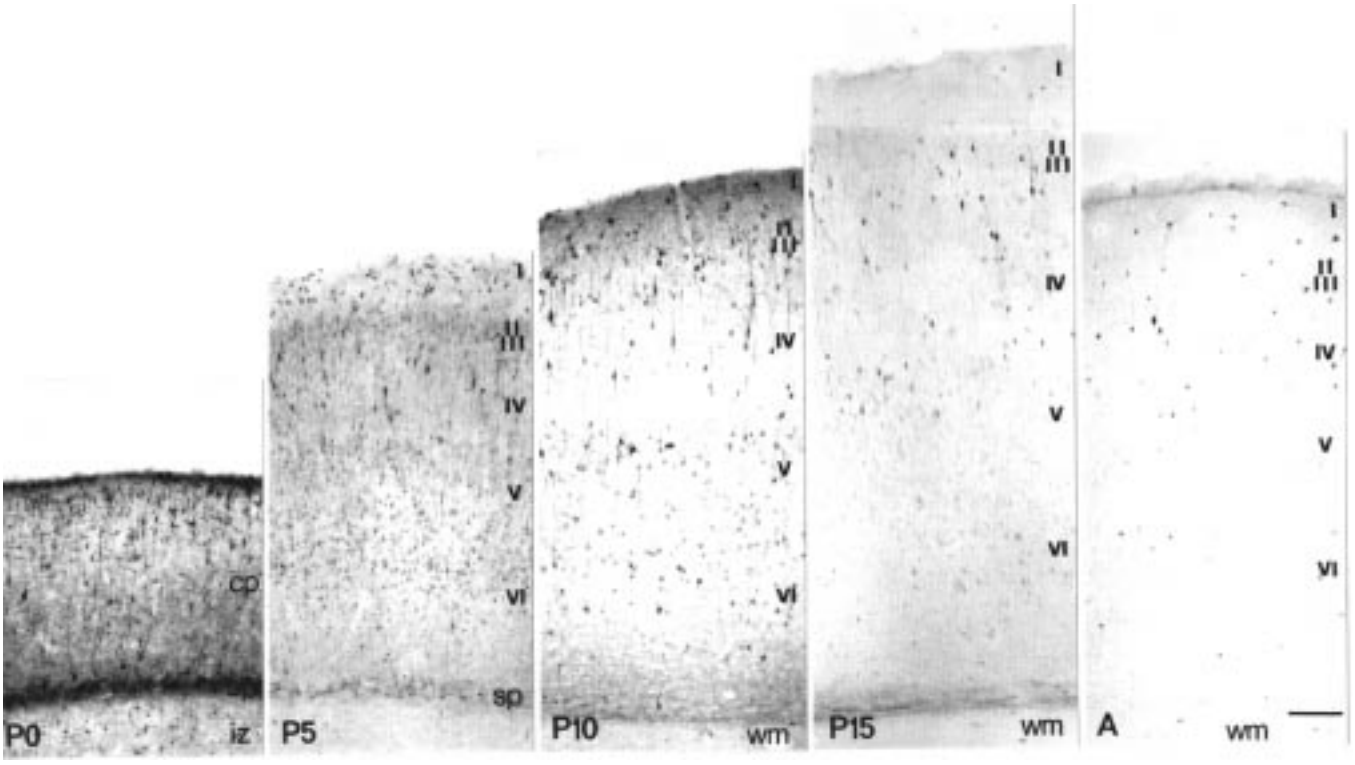

Figure 5. CR-immunoreactivity in the *occipital* region of rat isocortex on the day of birth (P0), on postnatal days 5 (P5), 10 (P10) and 15 (P15), and in the adult (A). cp = cortical plate; sp = subplate; wm = white matter; cortical layers (I–VI) are indicated. Scale bar = 120 μm.

on P20, but these had disappeared by P30. Sparsely distributed neurons could be detected in layer I and in the white matter (Fig. 7*B*,*C*), those in the former being horizontally oriented. Neuropil staining was discrete in all layers.

Quantitative Analysis of the Immunoreactive Neurons

In order to verify the qualitative impressions derived by morphological inspection, we counted CR-immunoreactive neurons throughout the entire depth of the cortex within the frontal-, parietal- and occipital region of the neocortex at P0, P5, P10, P15, P20 and P30, and in the adult (Table 1 and 2 and Fig. 8). Each region manifested the same temporal dynamics in the development of CR-immunoreactivity. During the first 10 postnatal days, a marked increase in the density of CR-immunoreactive cells was observed. The peak values were attained at P10. During the ensuing 5 days the densities of CR-immunoreactive neurons decreased dramatically, falling even below that seen on P0. Thereafter, densities remained constant into adulthood. Counts made within the parietal region of P20-rat sections incubated with an alternative polyclonal antiserum (a gift of J. Rogers; Rogers, 1987) gave virtually the same results [CR 7969: 389 ± 56 cells/mm^3 (mean ± SEM); CR_{Rogers}: 354 ± 38 cells/mm^3; $P = 0.62$ (Mann–Whitney *U*-test)].

Highly significant differences between cortical regions were observed only on P5 and P10 in the occipital- and parietal region (Table 3), densities being higher in the former. This difference became apparent by P5 but was highest at P10. On P10, the density of CR-immunoreactive cells in the occipital region was also significantly higher than that in the frontal one. These results confirmed the qualitative observations, that differences between cortical regions are most pronounced during the second postnatal week within neocortices of 10-day-old rats.

Immunoblotting

Immunoblot analyses of rat cortices using the antiserum CR 7969 revealed two immunoreactive bands (Fig. 9): one migrating with an apparent molecular weight of 29 kDa, which corresponded to the migration characteristics of purified recombinant human CR (lane A), and another with an apparent molecular weight of 36–38 kDa. The intensity of the band at 29 kDa increased during postnatal development, peaking between P10 and P20, whereas that of the other continued to increase steadily throughout the entire postnatal period monitored. Both bands were also visible under calcium-free conditions (data not shown).

ELISA

The polyclonal antiserum, raised in goats against CR used as coating antibody for the ELISA, has been shown by immunoblotting to detect a band at 29 kDa, which corresponds to that of purified recombinant human CR. No immunoreactivity was detected at 36–38 kDa (J.-C. Gander, unpublished observations). The CR content of isolated cortices increased during the first two postnatal weeks and peaked on P10 (Table 4, Fig. 10). At birth (P0) the CR content was 160 ± 50 pg CR/μg total soluble protein and this increased to 410 ± 120 pg CR/μg total soluble protein at P15. Thereafter, this parameter decreased slightly until the adult level (310 ± 80 pg CR/μg total soluble protein) was achieved.

Discussion

In the present study we have described the expression of CR-immunoreactivity in five different regions of the rat neocortex during postnatal development. The density of stained neurons increased gradually from the day of birth until P10 and then decreased abruptly to adult levels. Immunoblotting and

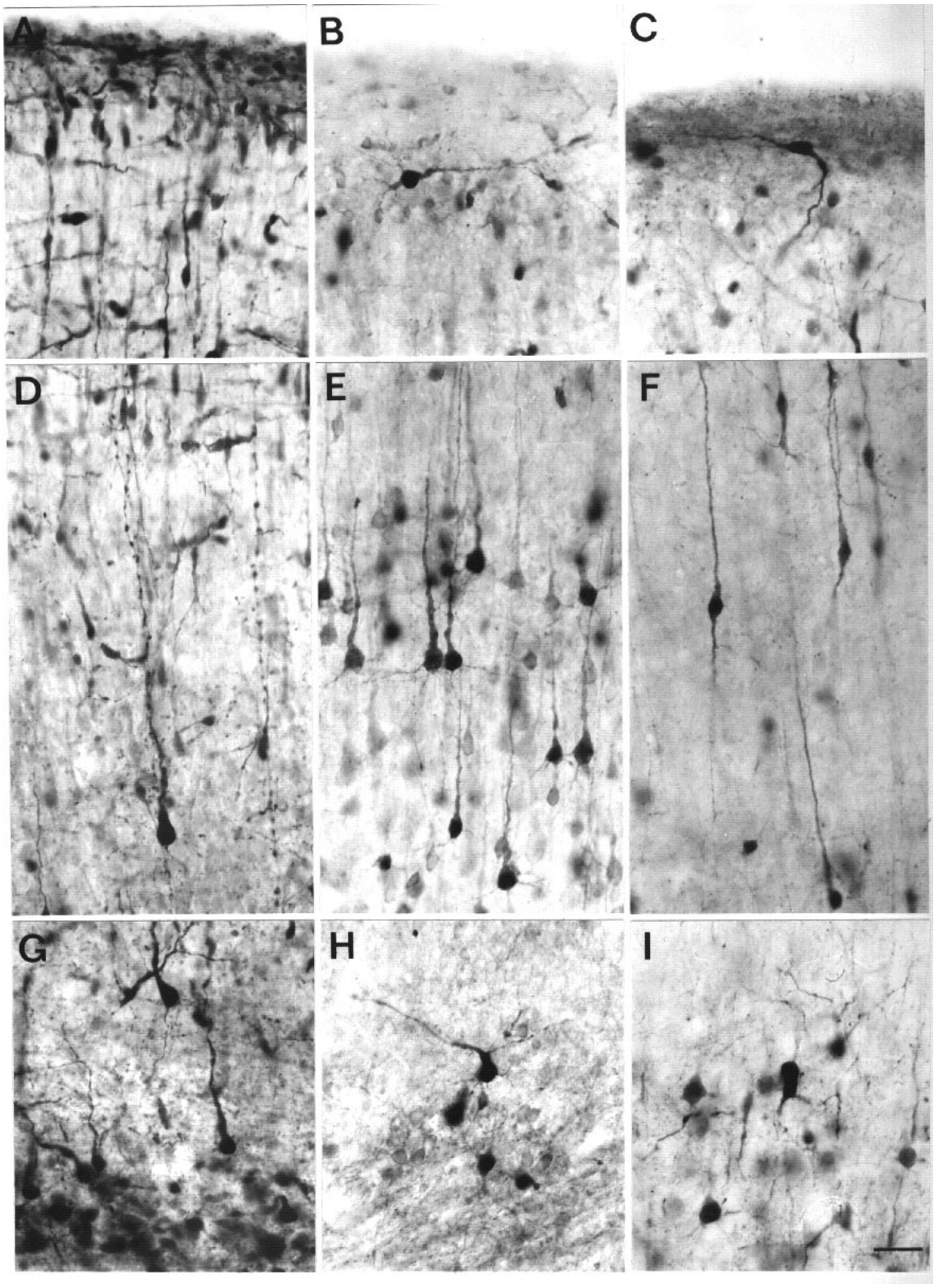

Figure 6. CR-immunoreactive neurons in rat isocortex on the day of birth (A, D, G) and on postnatal days 5 (B, E, H) and 10 (C, F, I). (A, B, C) CR-immunoreactivity in layer I. Many neurons exhibiting the morphology typical of Cajal–Retzius cells. (D, E) CR-immunoreactive pyramidal-like cells in the upper portion of layer V. (F) Bipolar and bitufted cells in the developing cortical plate. (G, H, I) CR-immunoreactivity in the subplate; note intense staining on the day of birth (G), which has virtually disappeared by day 10 (I). Scale bar = 60mm.

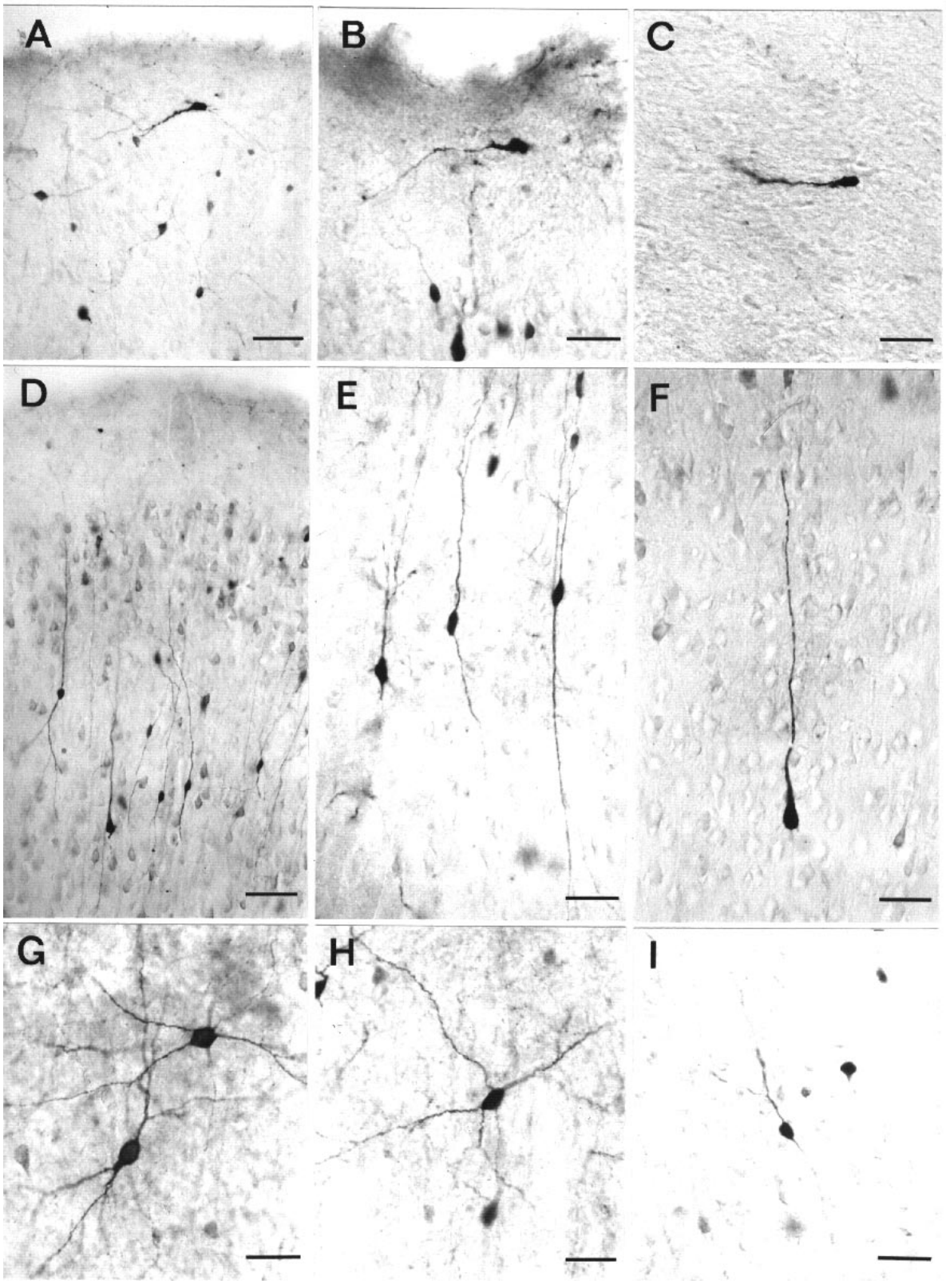

Figure 7. CR-immunoreactive neurons in rat isocortex on postnatal days 15 (*A*, *D*, *F*, *G*) and 30 (*E*, *H*) and in the adult (*B*, *C*, *I*). (*A*, *B*) CR-immunoreactive neurons in layer I of a 15-day-old (*A*) and an adult rat (*B*). (*C*) CR-immunoreactive neuron in the white matter underlying the frontal cortex of an adult rat. (*D*, *E*) CR-immunoreactive neurons in the supragranular layers of a 15-day-old (*D*) and a 30-day-old rat (*E*) exhibiting mainly bipolar and bitufted morphologies. (*F*) Pyramidal-like CR-immunoreactive neuron in the cingulate cortex of a 15-day-old rat. (*G*, *H*, *I*) Multipolar CR-immunoreactive neurons in the supragranular layers of a 15-day-old (*G*), a 30-day-old (*H*) and an adult rat (*I*).

Table 1
Number of calretinin-immunoreactive cells/mm^3 in the frontal, parietal and occipital regions of the rat neocortex

Postnatal age	Number of calretinin-immunoreactive cells/mm^3 (mean ± SEM)		
	Frontal region	Parietal region	Occipital region
P0	1152 ± 101	920 ± 30	883 ± 37
P5	1255 ± 108	900 ± 141	1819 ± 225
P10	2784 ± 178	1527 ± 202	3755 ± 182
P15	653 ± 63	467 ± 49	623 ± 100
P20	549 ± 70	389 ± 56	630 ± 115
P30	416 ± 34	394 ± 36	414 ± 27
Adult	368 ± 33	327 ± 25	476 ± 46

Table 2
Significant and non-significant differences (Mann–Whitney *U*-test) in the number of calretinin-immunoreactive cells between different postnatal ages in the frontal, parietal and occipital rat cortex

	Frontal region	Parietal region	Occipital region
P0 compared with			
P5	n.s.	n.s.	****
P10	****	**	****
P15	****	****	n.s.
P20	****	****	**
P30	****	****	****
Adult	****	****	****
P5 compared with			
P10	****	**	****
P15	****	**	****
P20	****	**	****
P30	****	****	****
Adult	****	****	****
P10 compared with			
P15	****	****	****
P20	****	****	****
P30	****	****	****
Adult	****	****	****
P15 compared with			
P20	n.s.	n.s.	n.s.
P30	**	n.s.	n.s.
Adult	****	n.s.	n.s.
P20 compared with			
P30	n.s.	n.s.	n.s.
Adult	n.s.	n.s.	n.s.
P30 compared with			
Adult	n.s.	n.s.	n.s.

****$P \leq 0.001$; **$0.001 \leq P \leq 0.05$; n.s., $P \geq 0.05$. Note that from P15 onwards differences between postnatal stages are not barely significant.

ELISA confirmed the impressions gleaned by morphological inspection and numerical analysis of immunostained tissue.

Immunoblotting and ELISA

Immunoblotting of neocortical extracts revealed the presence of a 36–38 kDa protein, in addition to the 29 kDa one characteristic of purified recombinant human CR (Schwaller *et al.*, 1993). The intensity of this additional immunoreactive band increased continuously from virtual absence on P0 to a level comparable to that manifested in the adult. An analogous situation has been reported for parvalbumin during postnatal development of the cat neocortex (Hogan and Berman 1993). Changes in the proportions of the two isoforms have been correlated with the onset of functional activity in the visual system. Such an interpretation cannot, however, account for the presence of the 36–38 kDa band, since it is expressed well before the onset of visually driven activity. This protein in the rat cortex may either

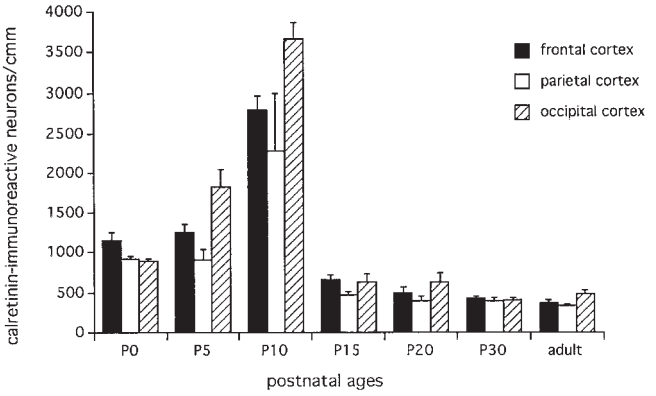

Figure 8. Histogram depicting the densities of CR-immunoreactive cells/mm^3 in different cortical regions (frontal, parietal and occipital) during development of the rat isocortex. Note the gradual marked increase in this parameter during the first 10 days and the sharp decline thereafter. Between postnatal day 15 and adulthood, the densities of CR-immunoreactive cells do not change significantly.

Table 3
Significant and non-significant differences (Mann–Whitney *U*-test) in the number of calretinin-immunoreactive cells between different cortical regions (frontal, parietal and occipital) of the rat cortex at different postnatal ages

	Postnatal age					
	P0	P5	P10	P15	P20	P30
Frontal region compared with						
Parietal region	n.s.	n.s.	**	n.s.	n.s.	n.s.
Occipital region	n.s.	n.s.	**	n.s.	n.s.	n.s.
Parietal region compared with						
Occipital region	n.s.	**	****	n.s.	n.s.	n.s.

****$P \leq 0.001$; **$0.001 \leq P \leq 0.05$; n.s., $P \geq 0.05$. Note that during development only in the second postnatal week are differences between cortical regions apparent.

be an isoform of CR which has undergone post-translational modification or may represent a dimer of the alternatively spliced form of CR (CR-22k) discovered in a colon carcinoma cell line (Schwaller *et al.*, 1995). The possibility of its reflecting an altered migration behaviour of CR itself due to conformational changes induced by a different calcium-binding status (Kuznicki *et al.*, 1995; Ikura, 1996; Winsky and Kuznicki, 1996) can be excluded, since this band persisted under calcium-free conditions. Therefore, further biochemical work must be done to elucidate the nature of the additional immunoreactive band in the rat cortex.

The existence of this immunoreactive band at 36–38 kDa in no way interfered with the results obtained by ELISA and immunocytochemistry. As a control for the specificity of CR 7969 in immunohistochemistry, we used a polyclonal antiserum against a chicken CR which does not detect additional isoforms (Rogers 1987; Belichenko *et al.*, 1995). The staining profile and numerical density counts thereby obtained were comparable to those achieved using the polyclonal antiserum CR 7969. This suggests that the two immunoreactive proteins most likely are colocalized in the same neurons. Furthermore, a polyclonal antiserum against goat CR was used as the coating antibody in the ELISA and this does not recognize the additional immunoreactive band. Therefore, using the ELISA technique only the full-length CR migrating at 29 kDa is detected.

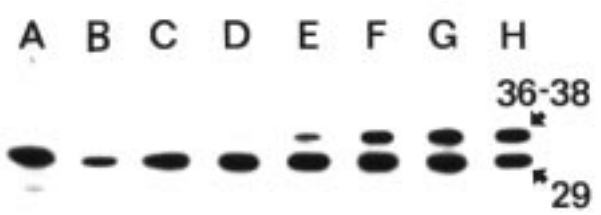

Figure 9. Immunoblot of rat isocortical extracts at different postnatal stages. Lane *A*: positive control: human recombinant CR. Lanes *B–H*: extracts of rat isocortices on the day of birth (*B*), on postnatal day 5 (*C*), 10 (*D*), 15 (*E*), 20 (*F*) and 30 (*G*), and of an adult rat (*H*). Note the presence of a second additional band in extracts of rat isocortices at an apparent molecular weight of 36–38 kDa from P5 onwards.

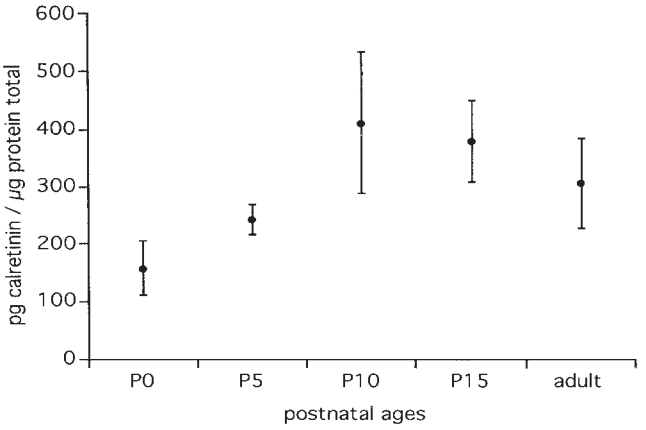

Figure 10. Quantitative analysis of CR content (pg/µg protein total) in the entire rat cortex during postnatal development.

Table 4
Amount of calretinin in pg/µg protein total in the developing cortex of the rat

Postnatal age	pg calretinin/µg total protein (mean ± SEM)
P0	160 ± 50
P5	240 ± 30
P10	410 ± 120
P15	380 ± 70
Adult	310 ± 80

The results of immunoblotting and the ELISA in general confirmed the immunocytochemical analysis. Both biochemical methods revealed an increase in the expression of CR during the second postnatal week, after which it decreased to adult levels. The level of CR expression in the adult isocortex is of the same magnitude as reported by Winsky and Jacobowitz (1991) for the insular cortex. The reduction in CR content recorded biochemically between P10 and adulthood was not, however, as pronounced as the decrease in the densities of CR-immunoreactive cells. Since a significantly enhanced staining intensity of the neuropil was not observed in elder rats, this cannot account for the discrepancy. A possible explanation is that in older animals, cells still exhibiting CR-immunoreactivity express this calcium-binding protein at higher levels than cells do at earlier phases of postnatal development. This hypothesis is supported by the observation that the proportion of intensely-to-faintly stained neurons appeared to increase towards adulthood. An alternative explanation could be that in older rats, CR exists mainly in a calcium-free conformation which is only weakly recognized by the antiserum employed (Winsky and Kuznicki, 1996). To exclude the possibility that neurons express CR which is not detected by the antiserum used, *in situ* hybridization in adult rat cortex is currently being performed.

Immunocytochemistry

The embryonic and postnatal development of CR-immunoreactivity in the parietal cortex of the rat has recently been described qualitatively (Vogt Weisenhorn *et al.*, 1994, 1996; Fonseca *et al.*, 1995). In the present study, we compared the postnatal pattern of development of CR-immunoreactivity in different regions of the cortex. CR-immunoreactive neurons were observed within all cortical layers from the first appearance of neurons onwards (Vogt Weisenhorn *et al.*, 1994; Del Río *et al.*, 1995; Fonseca *et al.*, 1995). The expression was marked during the first two postnatal weeks and diminished thereafter, with the definitive adult cell type specificity being achieved between the third and fourth postnatal weeks. This finding raises the question of whether CR-immunoreactive neurons are programmed to die during later phases of postnatal development, or whether specific neurons express CR-immunoreactivity transiently during the earlier phases.

Transient Labelling in Layer I

Judging from their morphological appearance, most of the CR-immunoreactive cells seen in layer I are Cajal–Retzius cells. These cells have been reported to die during postnatal development of the cortex (Derer and Derer, 1990; Del Río *et al.*, 1995). Hence, in the case of layer I the disappearance of CR-immunoreactive cells can be accounted for by natural cell death but probably not by apoptosis (Spreaficio *et al.*, 1995). There is evidence, however, that a small subset of CR-immunoreactive cells in layer I of rat and primate isocortex persists into adulthood (Condé *et al.* 1994; Vogt Weisenhorn *et al.*, 1994, 1996; Belichenko *et al.*, 1995; Fonseca *et al.*, 1995, Meyer *et al.*, 1995; Yan *et al.*, 1995a,b). These findings suggest that the population of the CR-immunoreactive neurons in layer I can be subdivided into different subpopulations according to their fate and probably also according to their functions. Recent reports have demonstrated that CR-immunoreactive neurons in layer I express a specific extracellular matrix protein which is involved in the organization of layers within the developing cortex (D'Arcangelo *et al.*, 1995, Ogawa *et al.*, 1995). It has yet to be determined whether the CR-immunoreactive cells surviving into adulthood also express this extracellular matrix protein. If they do not, they would represent a biochemically characterized and functional subclass of cells in layer I whose function has yet to be determined.

Transient Labelling in Layer V

Another readily identifiable class of cells expressing CR-immunoreactivity only transiently during postnatal development of the rat isocortex are cells displaying pyramidal morphology, located predominantly in the upper portion of layer V. A characteristic feature of typical pyramidal cells is the presence of spines, but these were lacking in the CR-immunoreactive neurons exhibiting pyramidal-like morphology. This could be due either to an insensitivity of the present method used or to the rare presence of spines on pyramidal neurons during the first two postnatal weeks. These cells could also belong to the non-spiny pyramidal-like cell population described in the prefrontal cortex of adult monkeys (Condé *et al.*, 1994). Still, according to their

dendritic morphology, we regard these cells as true pyramidal cells. However, whether these CR-immunoreactive pyramids are a morphologically and functionally distinct subpopulation of the population of pyramidal cells in layer V remains elusive. The disappearance of CR-immunoreactivity from this class of neurons at the end of the second postnatal week seems unlikely to be attributable to programmed cell death since this phenomenon is known to be accomplished already during the first postnatal week (Ferrer *et al.*, 1992, 1994; Spreafico *et al.*, 1995).

Transient staining of layer V pyramidal-like cells has also been reported for parvalbumin as well as for calbindin-D28k in both the kitten (Hogan and Bernam, 1993) and monkey (Hendrickson *et al.*, 1991; Spatz *et al.*, 1994). The functional significance of this phenomenon remains purely speculative. The distribution of CR-immunoreactive pyramidal neurons has been shown to be area-specific in all species thus far examined. That is, in motor regions and in the cingulate cortex more pyramidal neurons are stained than in purely sensory regions. Whether this distribution bears a relationship to the massive elimination of cortico-spinal projections which has been observed to occur during the second postnatal week (Stanfield and O'Leary, 1985) remains to be established.

Layer V of the rat cortex is also known to transiently express oestrogen receptor-immunoreactivity during the second week of development (Yokosuka *et al.*, 1995). This is of interest in the present context, since CR is known to be present in the steroid hormone-producing Leydig cells of the testis (Strauss *et al.*, 1994) as well as in interstitial cells of the ovary (Pohl *et al.*, 1992). However, whether there exists a relationship between these two observations remains to be determined.

Not only neurons but also the neuropil in the upper portion of layer V manifested marked CR-immunoreactivity. In the striate cortex of the neonatal new world monkey this region is highlighted by cytochrome oxidase staining and also by CR-immunoreactivity (Spatz *et al.*, 1993). The outer rim of layer V is a narrow and complex zone characterized by its own sets of neurons and axonal connections in the macaque, which suggests a specialized function within the striate cortex of primates (Lund, 1987). Our results indicate that also in the rodent cortex, layer Va has features distinct from those in Vb.

Correlations between the Developmental Pattern of CR-immunoreactivity and Developmental Processes

The spatial and temporal distribution profiles of the calcium-binding protein parvalbumin manifested in the cortex during development implicate its involvement in the final maturation of cortical circuits and/or the onset of experience-dependent activity. In contrast, CR-immunoreactivity is expressed very early during development and exhibited no major area specificity. Some minor regional differences were nonetheless observed on P10. The parietal cortex was distinguished by having a significantly lower number of CR- immunoreactive neurons than the frontal or occipital cortex and particularly by the presence of an intensely stained neuropil in the upper portion of layer V. The differences of the numbers do not reflect the general tendency of cortical development that the rostro-lateral regions mature slightly earlier than the more posterio-medial ones (Bayer and Altman, 1991; Ignacio *et al.*, 1995), indicating that the slight area differences are not due to general developmental events but to differences in the function of neuronal populations within these areas. However, the overall similarity in spatial and temporal CR-immunoreactivity distribution profiles between the regions examined supports the hypothesis that this calcium-binding protein is involved in fundamental developmental processes in corticogenesis.

Despite interspecies differences in the distribution profile of CR-immunoreactivity in adults (Jacobowitz and Winsky, 1991; Résibois and Rogers, 1992; Glezer *et al.*, 1992; Andressen *et al.*, 1993; Lund and Lewis, 1993; Lüth *et al.*, 1993; Condé *et al.*, 1994), the patterns manifested in the developing cortex of monkeys (Yan *et al.*, 1995a,b) and rats (Vogt Weisenhorn *et al.*, 1994, 1996; Fonseca *et al.*, 1995) are remarkably similar. It is present in both species very early in development and is maintained during the whole life. In both species there exists a specific period which is marked by a transient labelling of neurons. In the rat the density of CR-immunoreactive neurons is highest during the second postnatal week, whereas in monkey the peak of CR-immunoreactivity is in the late prenatal and early postnatal stages. It is interesting to note that these peaks correspond in both species to the end of neuronal migration and the onset of the final neuronal morphological maturation, i.e. exponential increase in the number of synapses, axonal and dendritic growth, and remodelling (Rakic, 1975; Blue and Parnavelas, 1983a,b; Miller, 1988; Bourgeois and Rakic, 1993; Ignacio *et al.*, 1995). This correlation strongly suggests an involvement of CR in these fundamental developmental processes, particularly since they are all calcium-dependent.

It should be borne in mind that our proposition for the involvement of CR in morphological differentiation holds true only for the temporal and spatial expression during the first three postnatal weeks of the development of the rat. During embryogenesis and in the adult rat, CR must necessarily be involved in different processes. It has been suggested that during embryogenesis CR may perhaps exert its buffering function on migrating neurons, which may need protection against elevated intracellular calcium concentrations (Vogt Weisenhorn *et al.*, 1994; Yan *et al.*, 1995a). The physiological importance of its expression in the cortex of adult rats also remains purely speculative.

Notes

We thank the following people for their helpful discussions and/or technical assistance: C. Dumas, B. Gotzos-Capelli, M. Rickman, E. S. Wintergerst, T. Pauls and B. Schwaller. We also thank Ms C. England for the correction of the manuscript. This study was supported by the Swiss National Science Foundation, Grant 3100.36483.92.

Correspondence should be addressed to Daniela M. Vogt Weisenhorn, Department of Anatomy and Cell Biology, Emory University, Atlanta, GA 30322, USA.

References

Alcántara S, Ferrer I, Soriano E (1993) Postnatal development of parvalbumin and calbindin D28k immunoreactivities in the cerebral cortex of the rat. Anat Embryol 188:63–73.

Alcántara S, Ferrer I (1994) Postnatal development of parvalbumin immunoreactivity in the cerebral cortex of the cat. J Comp Neurol 348:133–149.

Andressen C, Blümcke I, Celio MR (1993) Calcium-binding proteins: selective markers of nerve cells. Cell Tissue Res 271:181–208.

Bayer SA, Altman J (1991) Neocortical development. New York: Raven Press.

Belichenko PV, Vogt Weisenhorn DM, Myklóssy J, Celio MR (1995) Calretinin-positive Cajal–Retzius cells persist in the adult human neocortex. NeuroReport 6:1869–1874.

Blue ME, Parnavelas JG (1983a) The formation and maturation of synapses in the visual cortex of the rat. I. Qualitative analysis. J Neurocytol 12:599–616.

Blue ME, Parnavelas JG (1983b) The formation and maturation of synapses in the visual cortex of the rat. II. Quantitative analysis. J Neurocytol 12:697–712.

Bourgeois J-P, Rakic P (1993) Changes of synaptic density in the primary visual cortex of the macaque monkey from fetal to adult stage. J Neurosci 13:2801–2820.
Campbell AK (1983) Intracellular calcium:its universal role as regulator. In: Monographs in molecular biophysics and biochemistry (Gutfreund H, ed), pp 1–556. New York: Wiley.
Chard PS, Bleakman D, Christakos S (1993) Calcium buffering properties of calbindin D28k and parvalbumin in rat sensory neurons. J Physiol 472:341–357.
Choi DW (1988) Glutamate neurotoxicity and diseases of the nervous system. Neuron 1:623–634.
Condé F, Lund JS, Jacobowitz DM, Baimbridge KG, Lewis DA (1994) Local circuit neurons immunoreactive or calretinin, calbindin D-28k or parvalbumin in monkey prefrontal cortex: distribution and morphology. J Comp Neurol 341:95–116.
D'Arcangelo G, Miao GG, Chen S-C, Soares HD, Morgan JI, Curran T (1995) A protein related to extracellular matrix proteins deleted in the mouse mutant reeler. Nature 374:719–723.
Del Río JA, Martínez A, Fonseca M, Auladell C, Soriano E (1995) Wide distribution, glutamate-like immunoreactivity and fate of Cajal–Retzius cells in the developing murine cortex as identified with calretinin immunocytochemistry. Cereb Cortex 5:13–21.
Derer P, Derer M (1990) Cajal–Retzius cell ontogenesis and death in mouse brain visualized with horseradish peroxidase and electron microscopy. Neuroscience 36:839–856.
Enderlin S, Norman AW, Celio MR (1987) Ontogeny of the calcium-binding protein calbindin D-28k in the rat nervous system. Anat Embryol 177:15–28.
Ferrer I, Soriano E, Del Rio JA, Alcantara S, Auladell C (1992) Cell death and removal in the cerebral cortex during development. Prog Neurobiol 39:1–43F.
Ferrer I, Tortosa A, Blanco R, Martin F, Serrano T, Planas A, Macaya A (1994) Naturally occurring cell death in the developing cerebral cortex of the rat. Evidence of apoptosis-associated internucleosomal DNA fragmentation. Neurosci Lett 182:77–79.
Fonseca M, Del Río JA, Martínez a, Gómez S, Soriano E (1995) Development of calretinin immunoreactivity in the neocortex of the rat. J Comp Neurol 361:177–192.
Freund TF, Magloczky ZS (1993) Early degeneration of calretinin-containing neurons in the rat hippocampus after ischemia. Neuroscience 56:581–596.
Glezer II, Hof PR, Morgane PJ (1992) Calretinin-immunoreactive neurons in the primary visual cortex of dolphin and human brains. Brain Res 595:181–188.
Gotzos V, Schwaller B, Hetzel N, Bustos-Castillo M, Celio MR (1992) Expression of the calcium binding protein calretinin in WiDr cells and its correlation to their cell cycle. Exp Cell Res 202:292–302.
Hendrickson AE, Van Brederode JFM, Mulligan KA, Celio MR (1991) Development of calcium-binding proteins parvalbumin and calbindin in monkey striate cortex. J Comp Neurol 307:626–646.
Heizmann CW, Braun K (1995) Calcium regulation by calcium-binding proteins in neurodegenerative disorders. New York: Springer-Verlag.
Hof PR, Nimchinsky EA, Celio MR, Bouras C, Morrison JH (1993) Calretinin-immunoreactive neocortical interneurons are unaffected in Alzheimer's disease. Neurosci Lett 152:145–149.
Hogan D, Berman NEJ (1993) Transient expression of calbindin-D28k immunoreactivity in layer V pyramidal neurons during postnatal development of kitten cortical areas. Dev Brain Res 74:177–192.
Hogan D, Berman NEJ (1994) The development of parvalbumin and calbindin-D28k immunoreactive interneurons in kitten visual cortical areas. Dev Brain Res 77:1–21.
Hunziker W, Schrickel S (1988) Rat brain calbindin D-28K: six domain structure and extensive amino acid sequence homology with chick calbindin D-28K. Mol Endocrinol 2:465–473.
Iacopino AM, Quintero EM, Miller EK (1994) Calbindin-D28k: a potential neuroprotective protein. Neurodegeneration 3:1–20.
Ignacio MPD, Kimm EJ, Kageyama GH, Yu J, Robertson RT (1995) Postnatal migration of neurons and formation of laminae in rat cerebral cortex. Anat Embryol 191:89–100.
Ikura M (1996) Calcium binding and conformational response in EF-hand proteins. Trends Biochem 21:14–17.
Jacobowitz DM, Winsky L (1991) Immunocytochemical localization of calretinin in the forebrain of the rat. J Comp Neurol 304:198–218.
Kater SB, Mattson MP, Cohan C, Conner J (1988) Calcium regulation of the neuronal growth cone. Trends Neurosci 11:315–321.
Komuro H, Rakic P (1992) Selective role of N-type calcium channels in neuronal migration. Science 257:806–808.
Kuznicki J, Wang TCL, Martin BM, Winsky L, Jacobowitz DM (1995) Localization of calcium-dependent conformational changes of calretinin by limited tryptic proteolysis. Biochem J 308:607–612.
Lipton SA, Kater SB (1989) Neurotransmitter regulation of neuronal outgrowth, plasticity and survival. Trends Neurosci 12:265–270.
Liu F-Ch, Graybiel AM (1992) Transient calbindin-D28k-positive systems in the telencephalon: ganglionic eminence, developing striatum and cerebral cortex. J Neurosci 12:674–690.
Lukas W, Jones KA (1994) Cortical neurons containing calretinin are selectively resistant to calcium overload and excitotoxicity *in vitro*. Neuroscience 61:307–316.
Lund JS (1987) Local circuit neurons of macaque monkey striate cortex: I. Neurons of laminae 4C and 5A. J Comp Neurol 333:41–52.
Lund JS, Lewis DA (1993) Local circuit neurons of developing and mature macaque prefrontal cortex: Golgi and immunocytochemical characteristics. J Comp Neurol 328:282–312.
Lüth HJ, Blümcke I, Winkelmann E, Celio MR (1993) The calcium-binding protein calretinin is localized in a subset of interneurons in the rat cerebral cortex: a light and electron immunohistochemical study. J Hirnforsch 34:93–103.
Mattson MP, Kater SB (1987) Calcium regulation of neurite elongation and growth cone motility. J Neurosci 7:4034–4043.
Mattson MP, Kater SB (1989) Excitatory and inhibitory neurotransmitters in the generation and degeneration of hippocampal neuroarchitecture. Brain Res 478:337–348.
Mattson MP, Rychlik B, Chu C (1991) Evidence for calcium-reducing and excitoprotective roles for the calcium-binding protein calbindin-D28k in cultured hippocampal neurons. Neuron 6:41–51.
McDonald JW, Johnston MV (1990) Physiological and pathophysiological roles of excitatory amino acids during central nervous system development. Brain Res Rev 15:41–70.
Meyer G, Galindo-Mireles D, Carrillo-Padilla F, Ferres Torres R (1995) Calbindin, calretinin and NADPH-diaphorase in different cell classes in layer I of the adult human neocortex. Neurosci Abstr 21:794.1.
Miller MW (1988) Development of projection and local circuit neurons in neocortex. In: Cerebral cortex 7 (Peters H and Jones EG, eds) pp 133–175. New York: Academic Press.
Möckel V, Fischer G (1994) Vulnerability to excitotoxic stimuli of cultured rat hippocampal neurons containing the calcium-binding proteins calretinin and calbindin D-28k. Brain Res 648:109–120.
Ogawa M, Miyata T, Nakajima K, Yagyu K, Seike M, Ikenaka K, Yamamota H, Mikoshiba K (1995) The reeler gene-associated antigen on Cajal–Retzius neurons is a crucial molecule for laminar organization of cortical neurons. Neuron 14:899–912.
Parmentier M (1990) Structure of the human cDNAs and genes coding for calbindin-D28K and calretinin. In: Calcium-binding proteins in normal and transfected cells (Pochet R, Lawson DEM, Heizmann CW, eds), pp 27–34. New York: Plenum Press.
Pauls TL, Cox JA, Berchtold MW (1996) The calcium-binding proteins parvalbumin and oncomodulin and their genes: new structural and functional findings. Biochim Biophys Acta, in press.
Pohl V, Van Rampelbergh J, Mellaert S, Permentier M, Pochet R (1992) Calretinin in rat ovary: an *in situ* hybridization and immunohistochemical study. Biochim Biophys Acta 1160:87–94.
Rakic P (1975) Timing of major ontogenetic events in the visual cortex of the rhesus monkey. In: Brain mechanisms in mental retardation (Buchwald NA, Brazier M, eds), pp 3–40. New York: Academic Press.
Résibois A, Rogers JH (1992) Calretinin in rat brain: an immunohistochemical study. Neuroscience 46:101–134.
Rogers JH (1987) Calretinin: a gene for a novel calcium-binding protein expressed principally by neurons. J Cell Biol. 105:1343–1353.
Sánchez MP, Frassoni C, Alvarez-Volado G, Spreafico R, Fairén A (1992) Distribution of calbindin and parvalbumin in the developing cortex and its primordium in rat: an immunohistochemical study. J Neurocytol 21:717–736.
Schwaller B, Buchwald P, Blümcke I, Celio MR, Hunziker W (1993) Characterization of a polyclonal antiserum against the purified human recombinant calcium binding protein calretinin. Cell Calcium 14:639–648.
Schwaller B, Celio MR, Hunziker W (1995) Alternative splicing of calretinin mRNA leads to different forms of calretinin. Eur J Biochem 230:424–430.
Seto-Oshima A, Aoki E, Semba R, Emson PC, Heizmann CW (1990)

Appearance of parvalbumin-specific immunoreactivity in the cerebral cortex and hippocampus of the developing rat and gerbil brain. Histochemistry 94:579–589.

Solbach S, Celio MR (1991) Ontogeny of the calcium binding protein parvalbumin in the rat nervous system. Anat Embryol 184:103–124.

Spatz WB, Vogt DM, Illing R-B (1993) Distribution of cytochrome oxidase in layers IV and V of the striate cortex in neonate monkeys. Exp Brain Res 95:183–186.

Spatz WB, Illing R-B, Vogt Weisenhorn DM (1994) Distribution of cytochrome oxidase and parvalbumin in the primary visual cortex of the adult and neonate monkey, *Callithrix jacchus*. J Comp Neurol 339:519–534.

Spitzer NC, Gu X, Olson E (1994) Action potentials, calcium transients and the control of differentiation of excitable cells. Curr Opin Neurobiol 4:70–77.

Spreafico R, Frassoni C, Arcelli P, Selvaggio M, De Biasi S (1995) *In situ* labelling of apoptotic cell death in the cerebral cortex and thalamus of rats during development. J Comp Neurol 363:281–295.

Stanfield BB, O'Leary DDM (1985) The transient corticospinal projection from the occipital cortex during the postnatal development of the rat. J Comp Neurol 238:236–248.

Stichel CC; Singer W, Heizmann CW (1987) Immunohistochemical localization of calcium binding proteins, parvalbumin and calbindin-D28k, in the adult and developing visual cortex of cats: a light and electron microscopic study. J Comp Neurol 262:563–577.

Strauss KI, Isaacs KR, Ha QN, Jacobowitz DM (1994) Calretinin is expressed in the Leydig cells of rat testis. Biochim Biophys Acta 1219:435–440.

Vogt Weisenhorn DM, Weruaga Prieto E, Celio MR (1994) Localization of calretinin in cells of layer I (Cajal–Retzius cells) of the developing cortex of the rat. Dev Brain Res 82:293–297.

Vogt Weisenhorn DM, Weruaga Prieto E, Celio MR (1996). Calretinin-immunoreactivity in organotypic cultures: effect of serum deprivation. Exp Brain Res 108:101–112.

Williams RW, Rakic P (1988) Three-dimensional counting: an accurate and direct method to estimate numbers of cells in sectioned material. J Comp Neurol 278:344–352.

Williams RW, Rakic P (1989) Three-dimensional counting: an accurate and direct method to estimate numbers of cells in sectioned material. J Comp Neurol 281:335.

Winsky L, Jacobowitz DM (1991) Radioimmunoassay of calretinin in the rat brain. Neurochem Int 19:517–522.

Winsky L, Kuznicki J (1996) Antibody recognition of calcium-binding proteins depends on their calcium-binding status. J Neurochem 66:764–771.

Yan Y-H, Van Brederode JFM, Hendrickson AE (1995a) Developmental changes in calretinin expression in GABAergic and nonGABAergic neurons in monkey striate cortex. J Comp Neurol 363:78–92.

Yan Y-H, Van Brederode JFM, Hendrickson AE (1995b) Transient co-localization of calretinin, parvalbumin and calbindin-D28k in developing visual cortex of monkey. J Neurocytol 24:825–837.

Yokosuka M, Okamura H, Hayashi S (1995) Transient expression of estrogen receptor-immunoreactivity (ER-IR) in layer V of the developing rat cerebral cortex. Dev Brain Res 84:99–108.

Yuste R, Nelson DA, Rubin WW, Katz LC (1995) Neuronal domains in developing neocortex: mechanisms of coactivation. Neuron 14:7–17.

Zilles K, Wree A (1985) Cortex: areal and laminar structure. In: The rat nervous system (Paxinos E, ed), vol 1, pp 375–416. Academic Press, Australia.